Institute of Electron Microscopy and Nanoanalysis

Differential phase contrast scanning transmission electron microscopy (DPC-STEM)

What it is good for and why it is hyped within the community

Thomas Mairhofer

Supervisors: Ferdinand Hofer, Gerald Kothleitner

DocDay
03.10.2022

Outline

Electron Microscopy and the information one can usually gain

Differential Phase Contrast STEM

Chemical and magnetic structure of spinodal magnetic alloys

- $Cu_{52}Ni_{34}Fe_{14}$
- $Fe_{54}Cr_{31}Co_{15}$

Multiferroic (doped) Bismuth Ferrite

- structure, polarization domains and vacancies

Electron Microscopy

Signals of a STEM

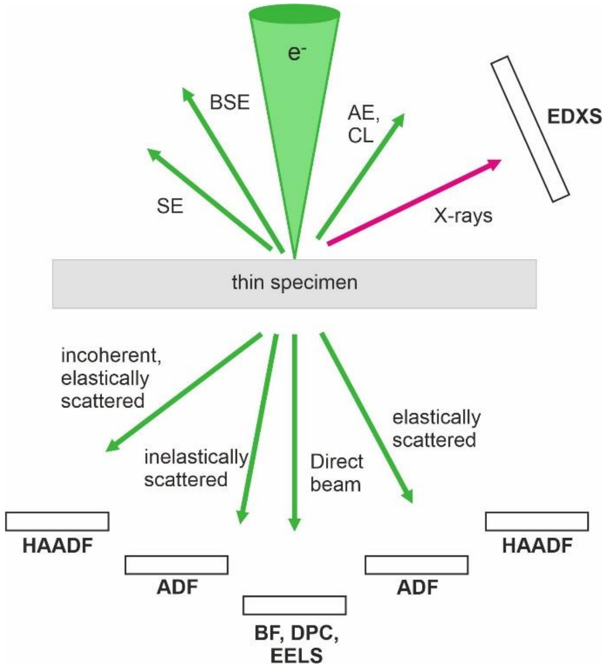

EDXS:

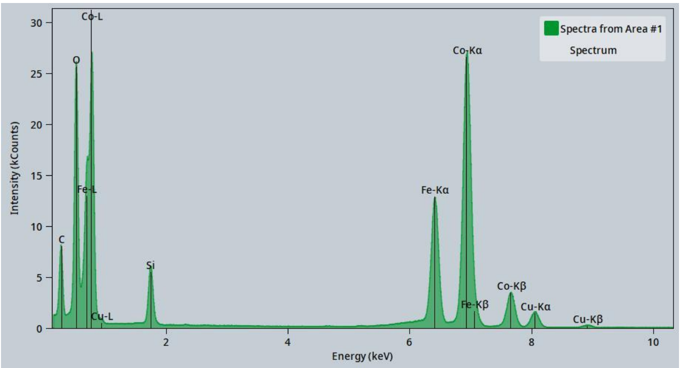

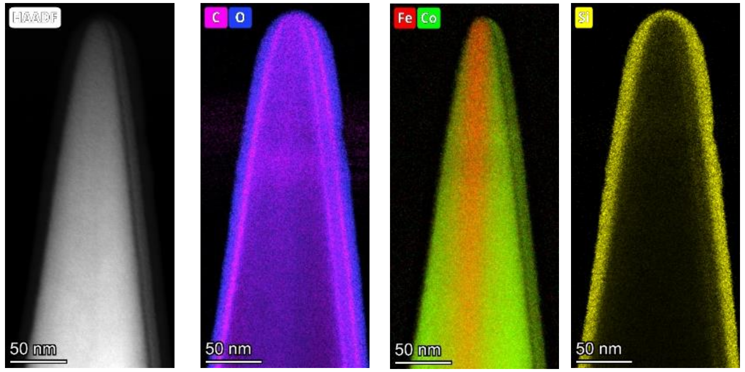

HAADF:

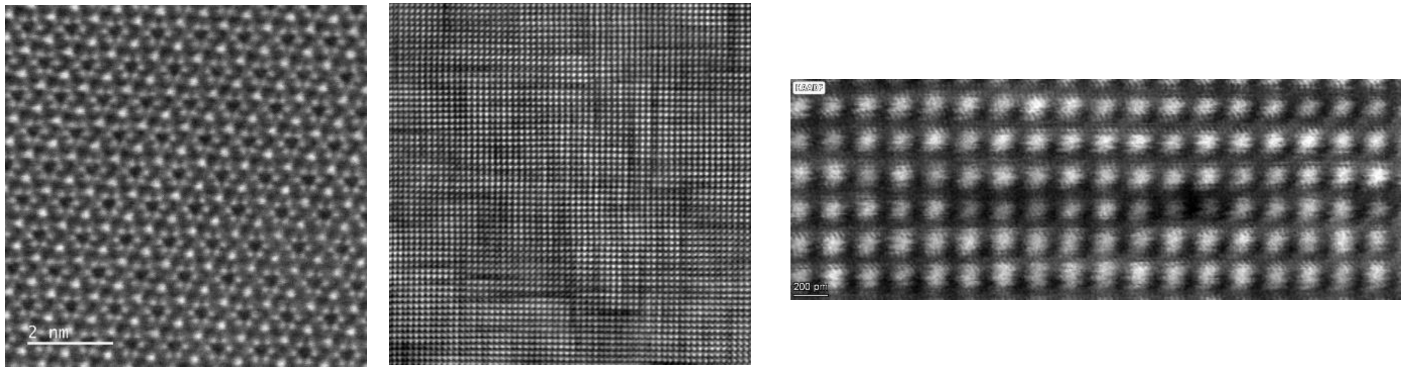

EELS:

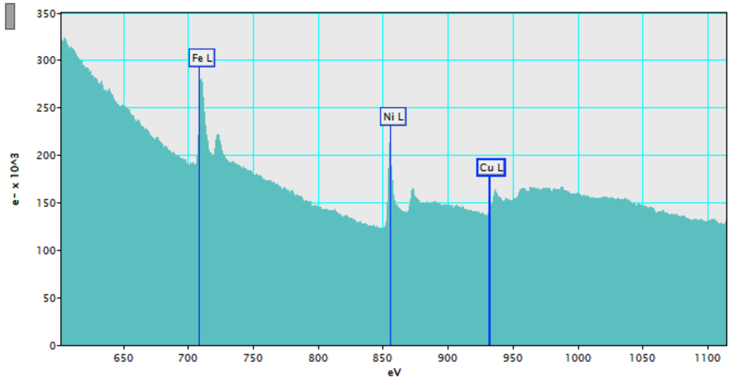

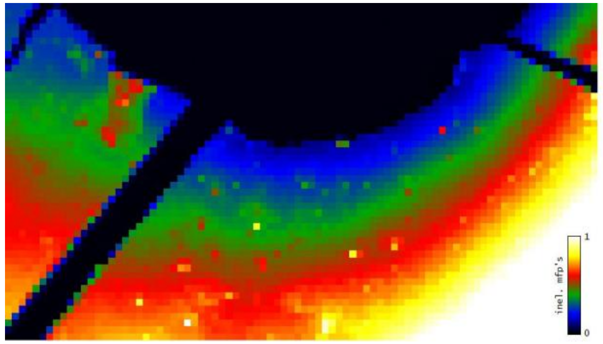

Differential Phase Contrast (DPC)-STEM

Open questions:

What about imaging electromagnetic fields?

How to image light elements?

Skyrmion lattice [8]

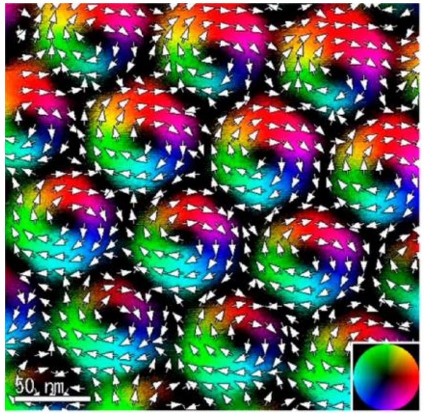

TiH [7]

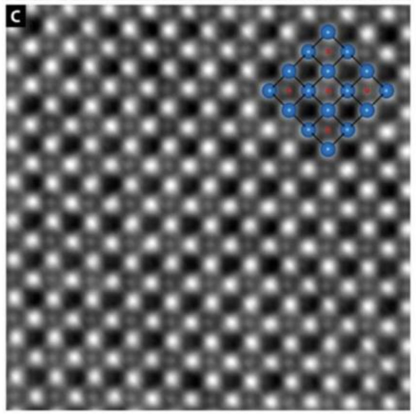

Magnetic domains
1978 [3]

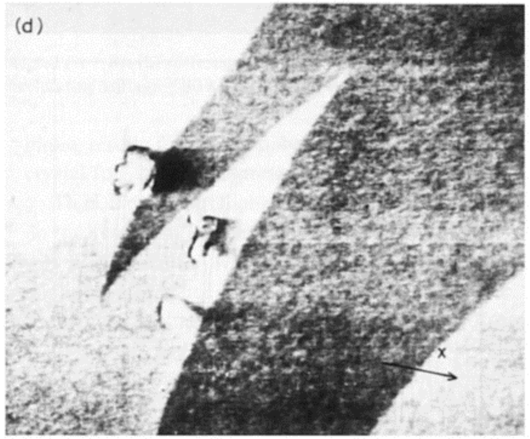

Electric field
2012 [4]

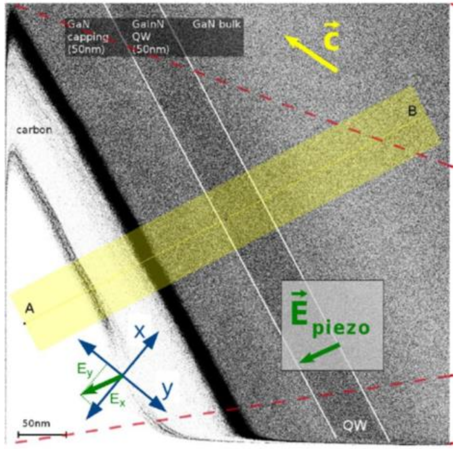

Atomic Electric fields
2012 [5]

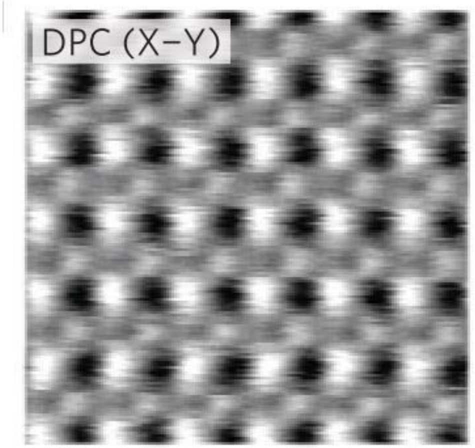

STO [6]

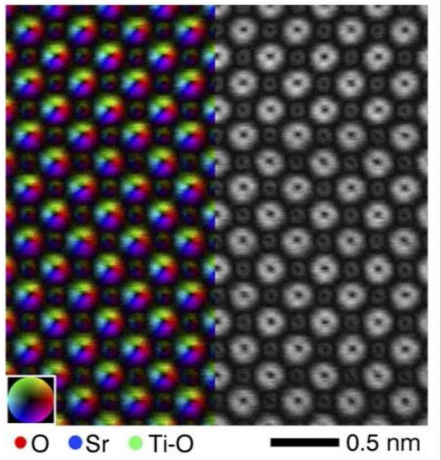

[3] Chapman et al. *Ultramicroscopy 3* (1978)
[4] Lohr et al. *Ultramicroscopy 117* (2012)
[5] Shibata et al. *Nature Physics 8* (2012)
[6] Shibata et al. *Nat. Commun.* 8 (2017)
[7] De Graaf et al. *Science Advances 6* (2020)
[8] Shibata et al. *Accounts of chemical research 50* (2017)

Principles of DPC-STEM

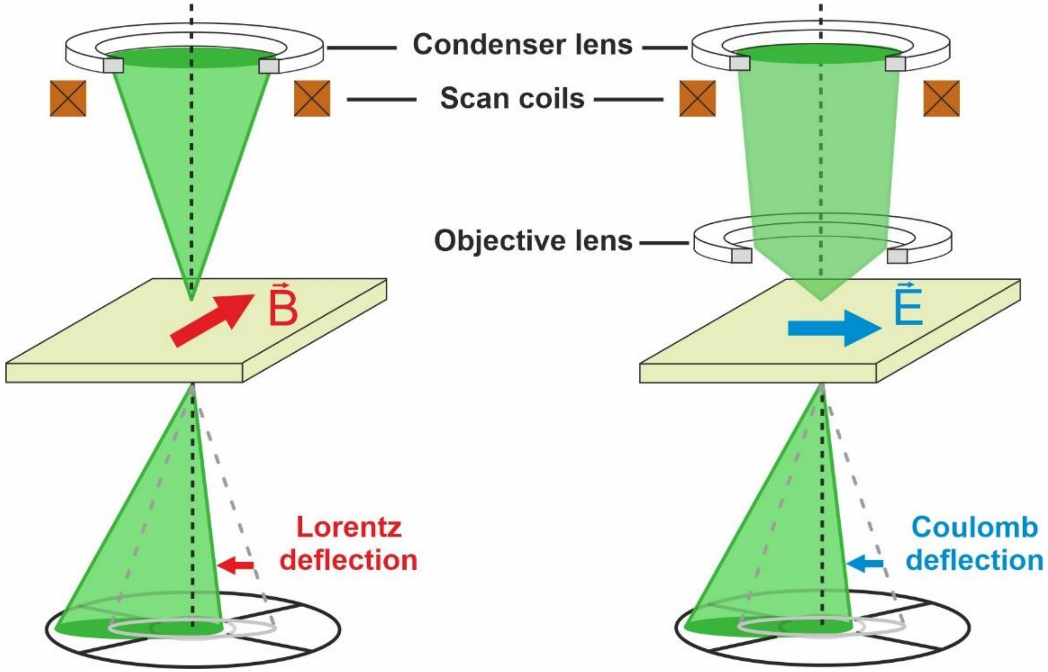

Classical approach

$$F_{Lorentz} = q(\vec{E} + (\vec{v} \times \vec{B}))$$

$$\beta_{mag} = -\frac{e\lambda}{h} Bs \qquad \beta_{elec} = \frac{e\lambda}{h\nu} Es \leftarrow \beta = \frac{1}{k}\nabla\varphi \leftarrow$$

Thin specimen -> Phase object approx.

$$\psi_{out}(r,t) = \psi_{in}(r,t) \cdot e^{i\varphi}$$

Shift = movement of CoM

$$I^{CoM} = <\hat{p}> = \int kI(k, r_p)d^2k = \int k|\psi(k, r_p)|^2 d^2k$$

$$= \frac{1}{2\pi}\left(|\psi_{in}(\vec{r})|^2 * \vec{\nabla}\varphi(\vec{r})\right)(\vec{r_p}) \quad [9]$$

DPC = approximation to CoM

$$I^{DPC} \approx I^{CoM} \propto \nabla\varphi$$

Phase of electron wave

$$\varphi = \frac{e}{\hbar\nu}\int V\,ds - \frac{e}{\hbar}\oint \vec{A}\,d\vec{s} = \frac{e}{\hbar\nu}\int V\,ds - \frac{e}{\hbar}\int_S \vec{B}\,d\vec{S}$$

[9] Lazic, Bosch and Lazar, *Ultramicroscopy 160* (2016)

Signal detection of DPC

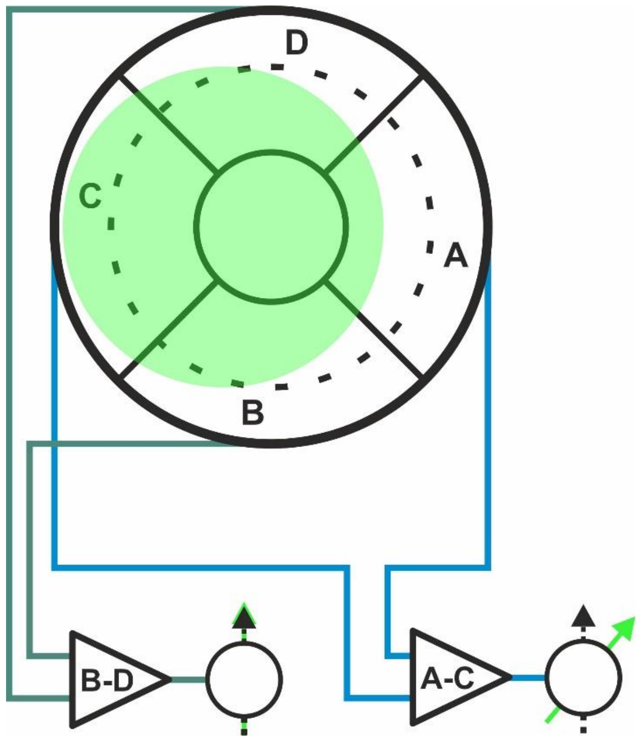

Sketch of a 4-quadrant detector which is used in this work

Example: Annular detector divided into 4 quadrants

Difference signal of opposing segments used to determine center of mass

2D deflection vector of every scanned position measured

Relation of deflection vector and field vectors known

Colorwheel representation a possibility to display 2D vectors: direction of vector plotted as function of hue (Farbton)

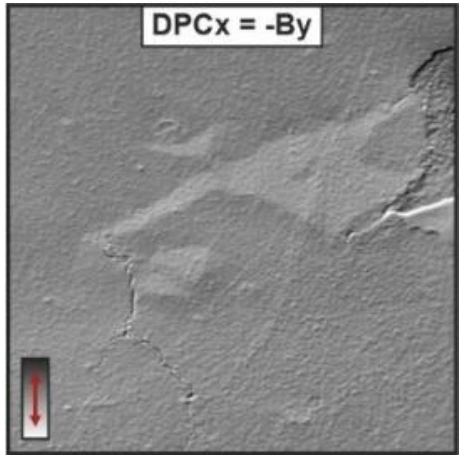

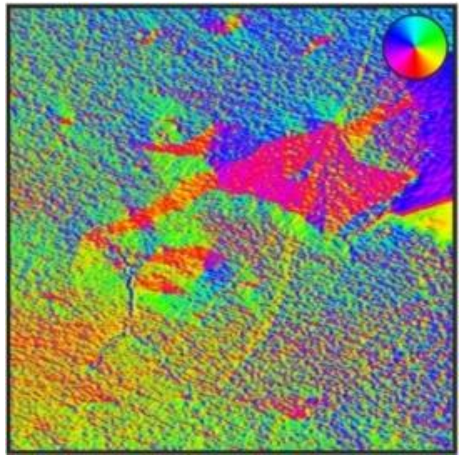

polycrystalline Co-film Specimen provided by Prof. Josef Zweck, Univ. Regensburg

[10] Zweck, *J. Phys.: Condens. Matter 28* (2016)

CuNiFe / spinodal alloys

Spinodal Decomposition

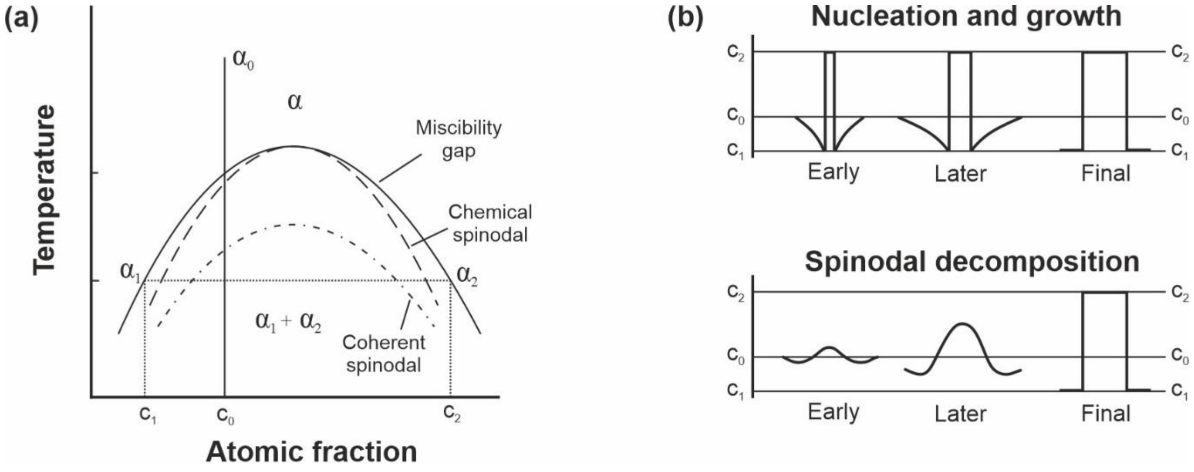

AlNiCo [13]

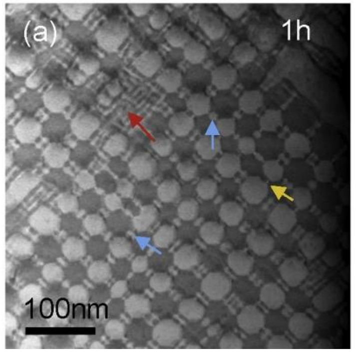

CuNiFe [14]

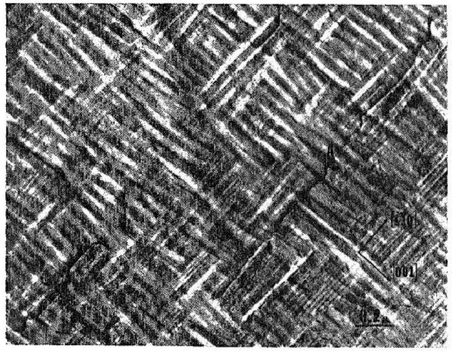

FeCoNiMnCu - HEA [15]

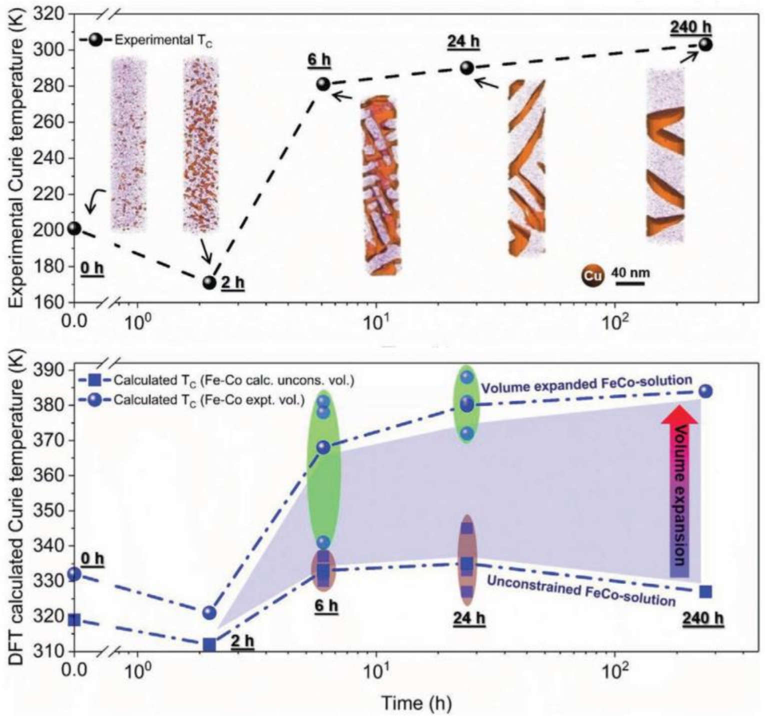

Advanteges of spinodal decomposition:

Uniform microstructure
Same crystal structure for both phases (at least in the beginning)
‚slow‘ process
Adds flexibility to tune physical properties (hardening, magnetism)

[12] Findik *Materials and Design 42* (2012)
[13] Zhou et al. *Acta Materialia 153* (2018)
[14] Butler and Thomas *Acta Metallurgica 18* (1970)
[15] Rao et al. *Advanced Functional Materials 7* (2020)

$Cu_{52}Ni_{34}Fe_{14}$ - chemical microstructure

EDXS elemental maps

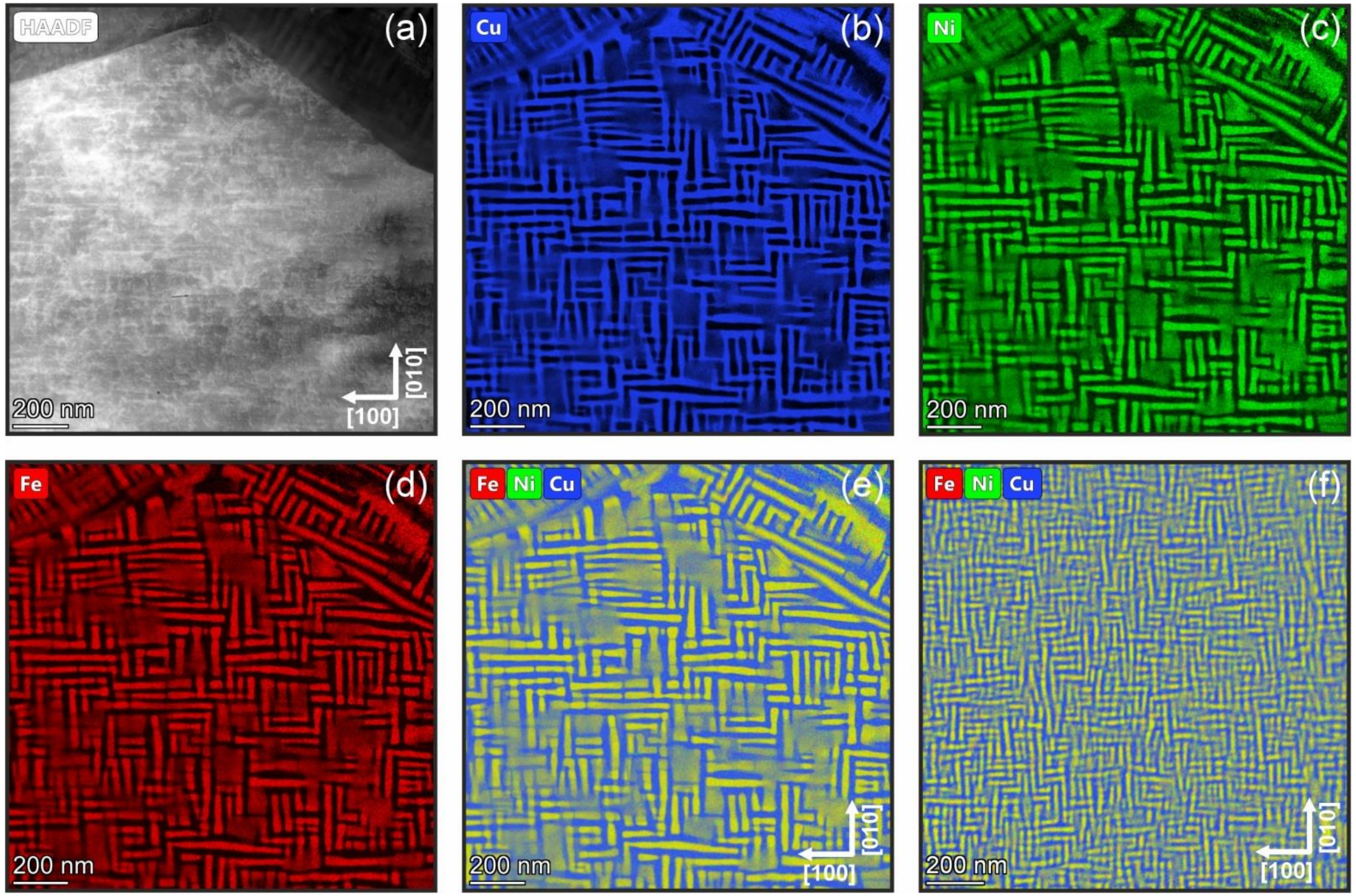

Spinodal decomposition @ 625°C

Segregation into NiFe-rich and Cu-rich phases

Platelet-like shape of NiFe-rich phase

Platelets along the <100> crystallographic directions

Size of platelets dependend on the heating duration

$Cu_{52}Ni_{34}Fe_{14}$ - DPC

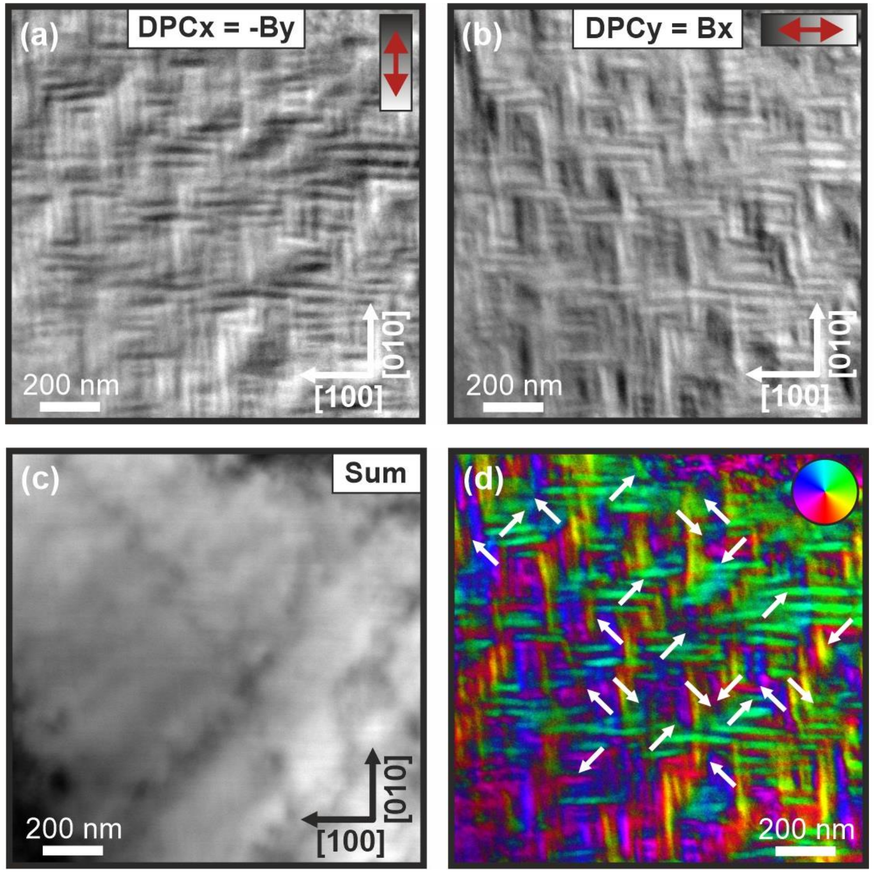

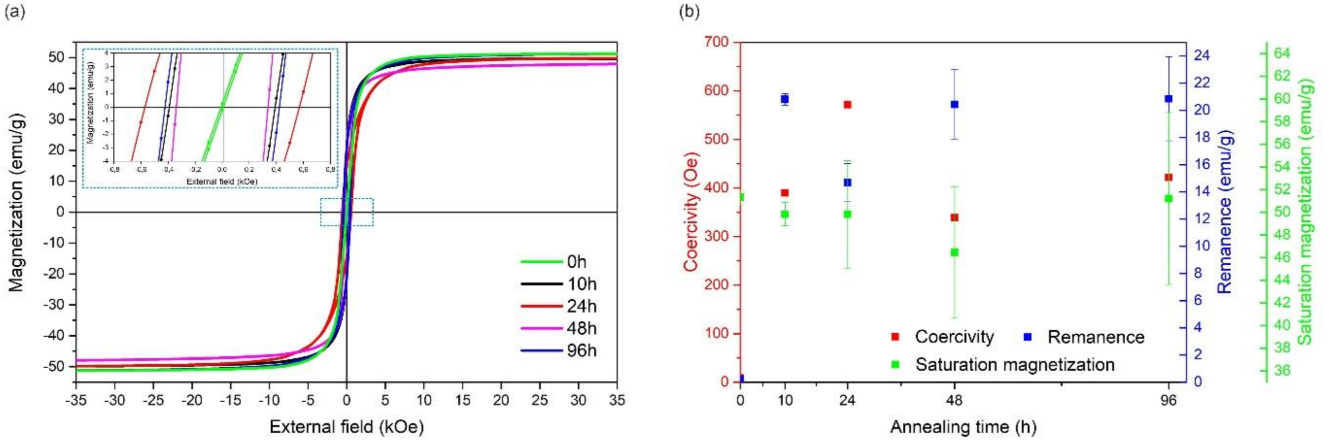

All aged CuNiFe alloys show ferromagnetism due to the formation of NiFe-rich platelets

DPC difference images reveal block-like domain structure

DPC induction map (colorwheel rep.) reveals the magnetization vectors within a domain along the diagonals

<111> was found to be the magnetic easy axis

[16] Radlinger et al. *Journal of alloys and compounds 922* (2022)

$Fe_{54}Cr_{31}Co_{15}$ - chemical structure

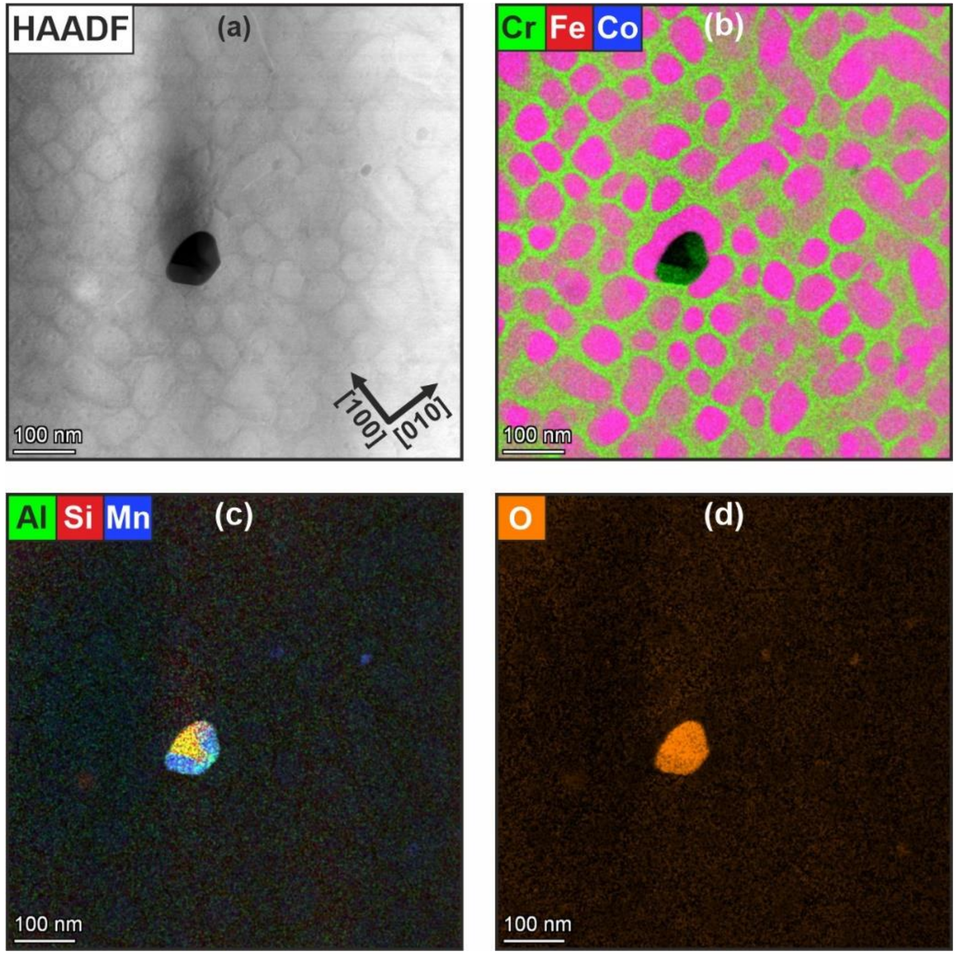

EDXS quant.	Fe / at%	Cr / at%	Co / at%
Overall	54	31	15
FeCo-rich	69	8	23
Cr-rich	36	57	7

HAADF image reveals three different phases due to different contrast (Z-contrast).

EDXS elemental maps reveal FeCo-rich particles embedded in a Cr-rich matrix

Cuboid FeCo-rich particles show tendency to align edges along the <100> crystallographic directions

Al/Si/Mn-Oxide inclusions due to additive manufacturing and *in-situ* alloying process

[17] Mairhofer et al. *In preparation*

$Fe_{54}Cr_{31}Co_{15}$ - magnetic structure

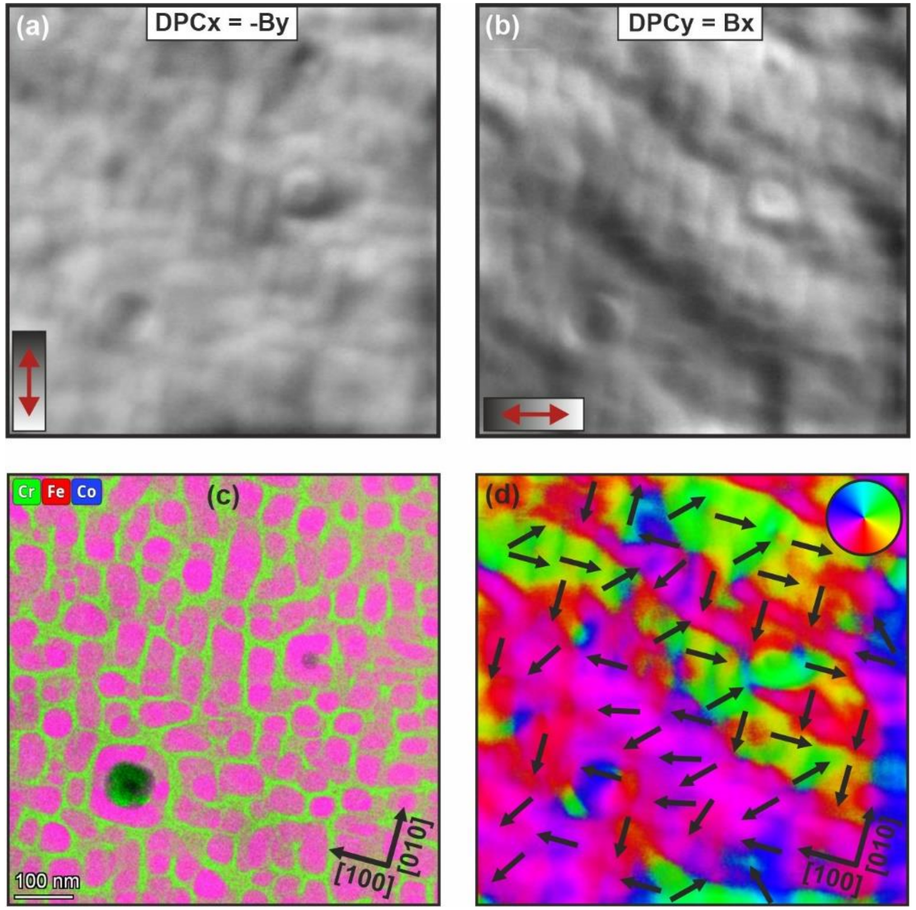

Sample #	Laser Power / W	Energy Density / J/cm²	Homogenisation	Heat treatment	$\mu_0 H_c$ (kA/m)	$\mu_0 M_r$(T)	BH_{max} (kJ/m³)
1	240	400	No	640HT	22.29	0.42	0.08
2	240	400	1100°C	640HT	19.10	0.47	0.08
3	240	400	1100°C	510HT	0.80	0.10	0.08

lamellar shaped magnetic domain structure visible

Several FeCo-particles couple to form domains

Weak correlation between chemical and magnetic structure

Tendency of magnetization pointing along the <100> directions. (in agreement to literature of FeCo-rich phase)

[17] Mairhofer et al. *In preparation*

Bismuth Ferrite

Structure model of $BiFeO_3$ (BFO)

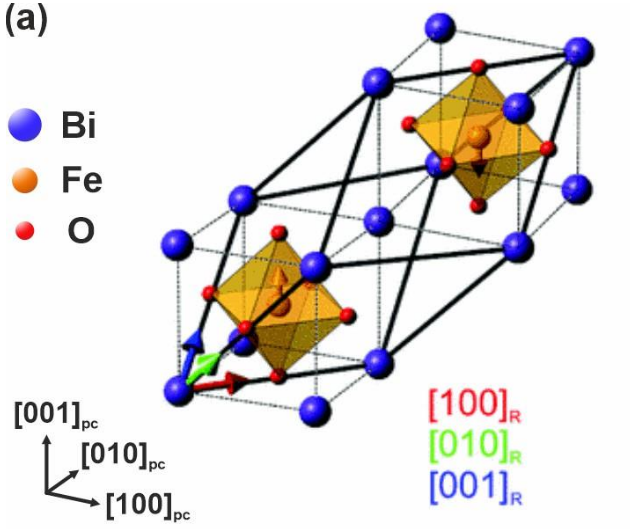

ferroelectric + antiferromagnetic
pseudocubic crystal structure
doping can change physical properties.
Can we use STEM (DPC) to map it?

High resolution images of BFO on SRO/STO substrate

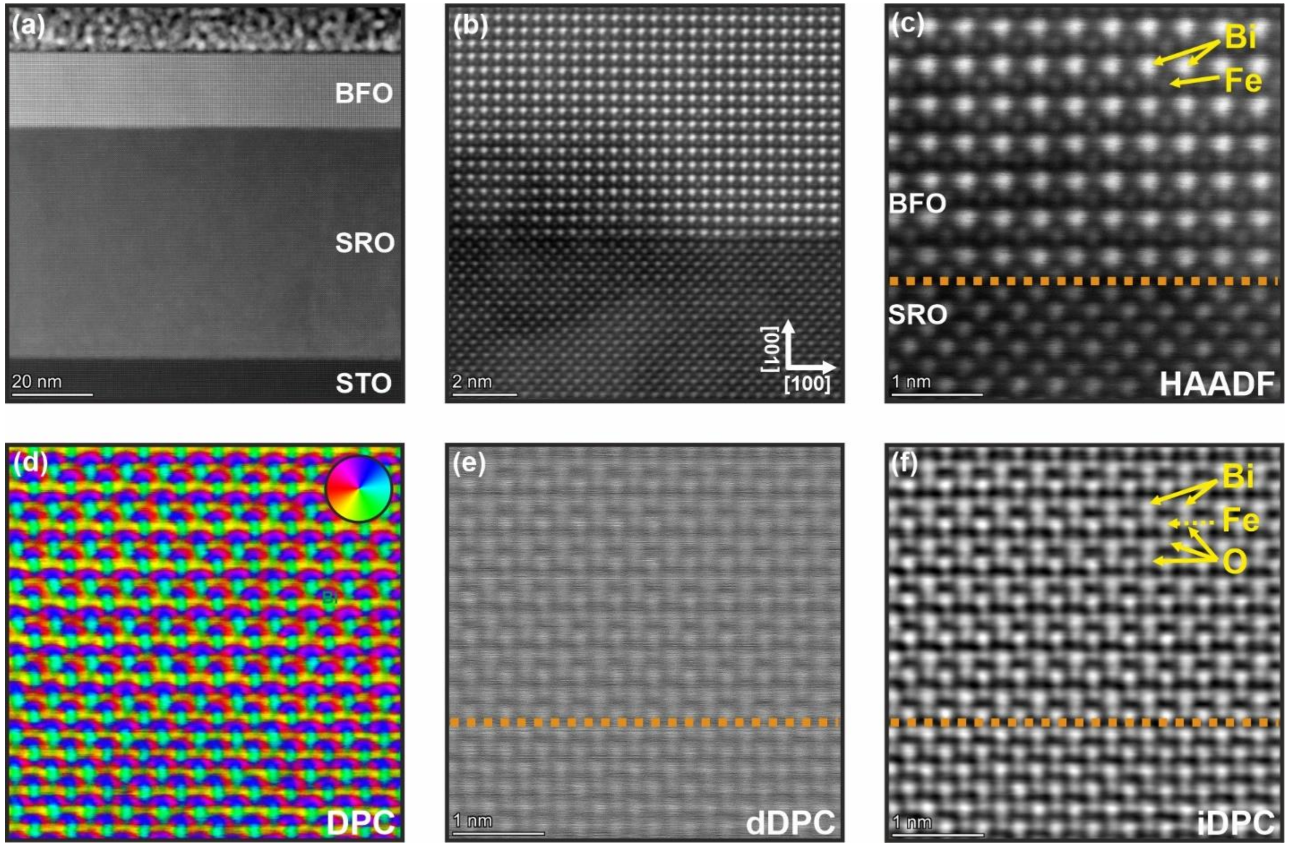

$I^{DPC} \propto \nabla\varphi = \vec{E}$ → *differentiating* → $I^{dDPC} \propto \nabla^2\varphi = \rho$

$\boldsymbol{I^{iDPC} \propto \varphi = V}$ (*integrating* from I^{DPC})

$$\nabla^2 V = \nabla\vec{E} = \frac{1}{\epsilon_0}\rho$$

doped BFO (BCFMO)

Specimen:
co-doped BFO with Ca and Mg - $\mathbf{Bi_{0.8}Ca_{0.2}Fe_{0.95}Mg_{0.05}O_3}$

HAADF + EELS

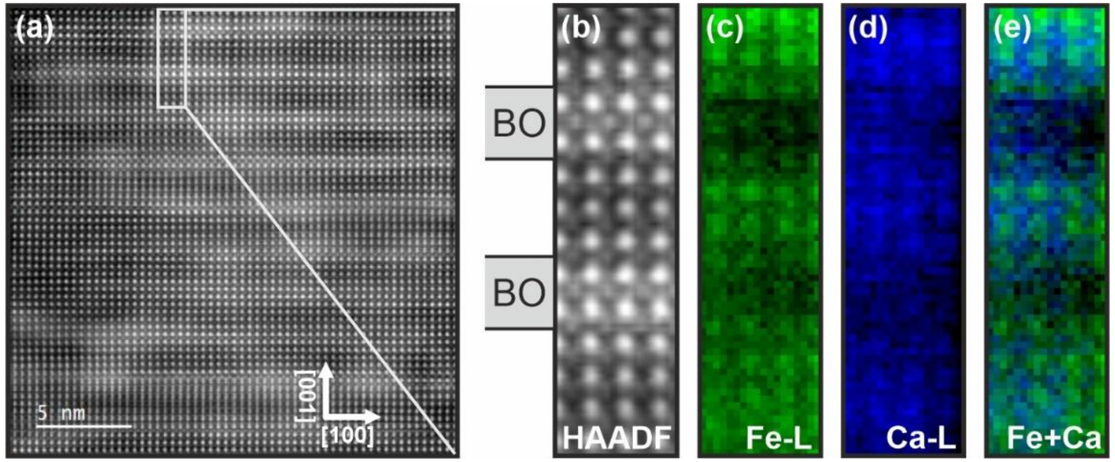

HAADF + EDXS elemental maps

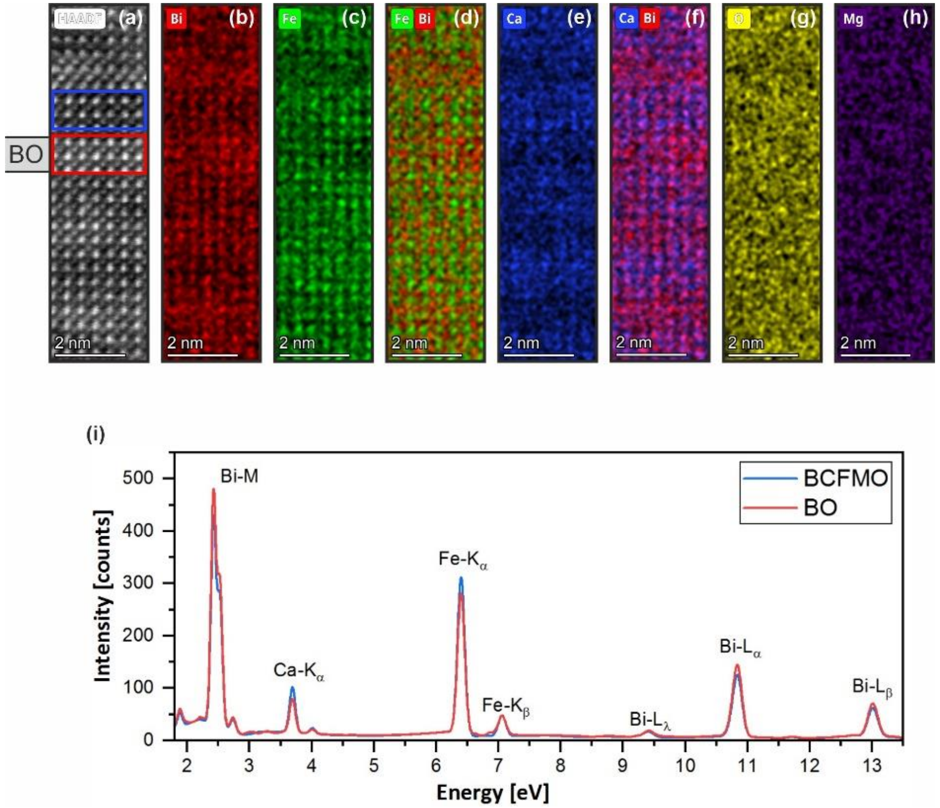

Doping causes bright layers

Lattice enlargement, EELS/EDXS elemental maps and DFT calculations revealed formation of a secondary BO-phase

[18] Haselmann, Radlinger et al. *J. Phys. Chem. C 126* (2022)

Mapping polarization domains of BCFMO

Imaging the ferroelectric polarization

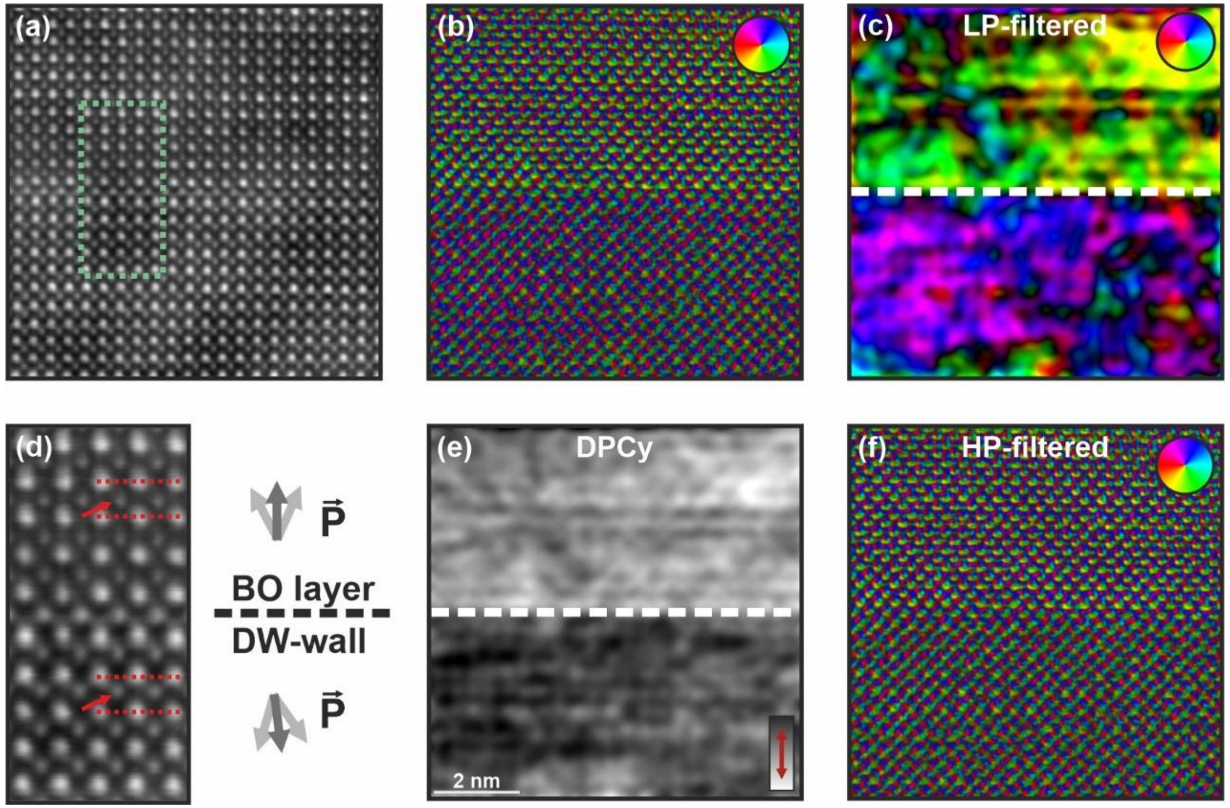

Determining the ferroelectric polarization either by the displacement of Fe atoms or with DPC

Sudden color change in DPC image indicates polarization domainwall at BO-secondary plate

Filtering of DPC images enhances contrast

Matching results of displacement/DPC analysis

O-vacancies within BCFMO

Cutout of an iDPC image

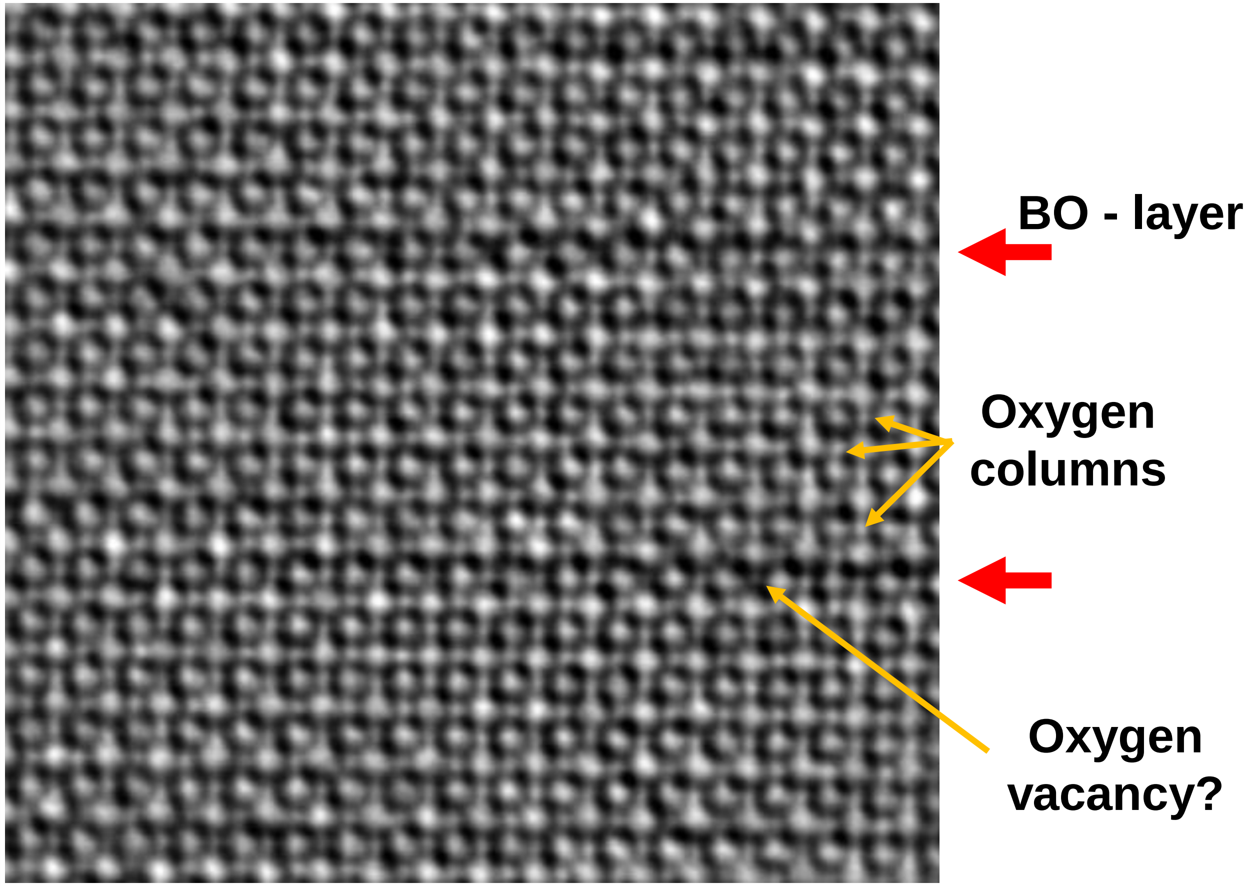

Imaging the O-vacancies

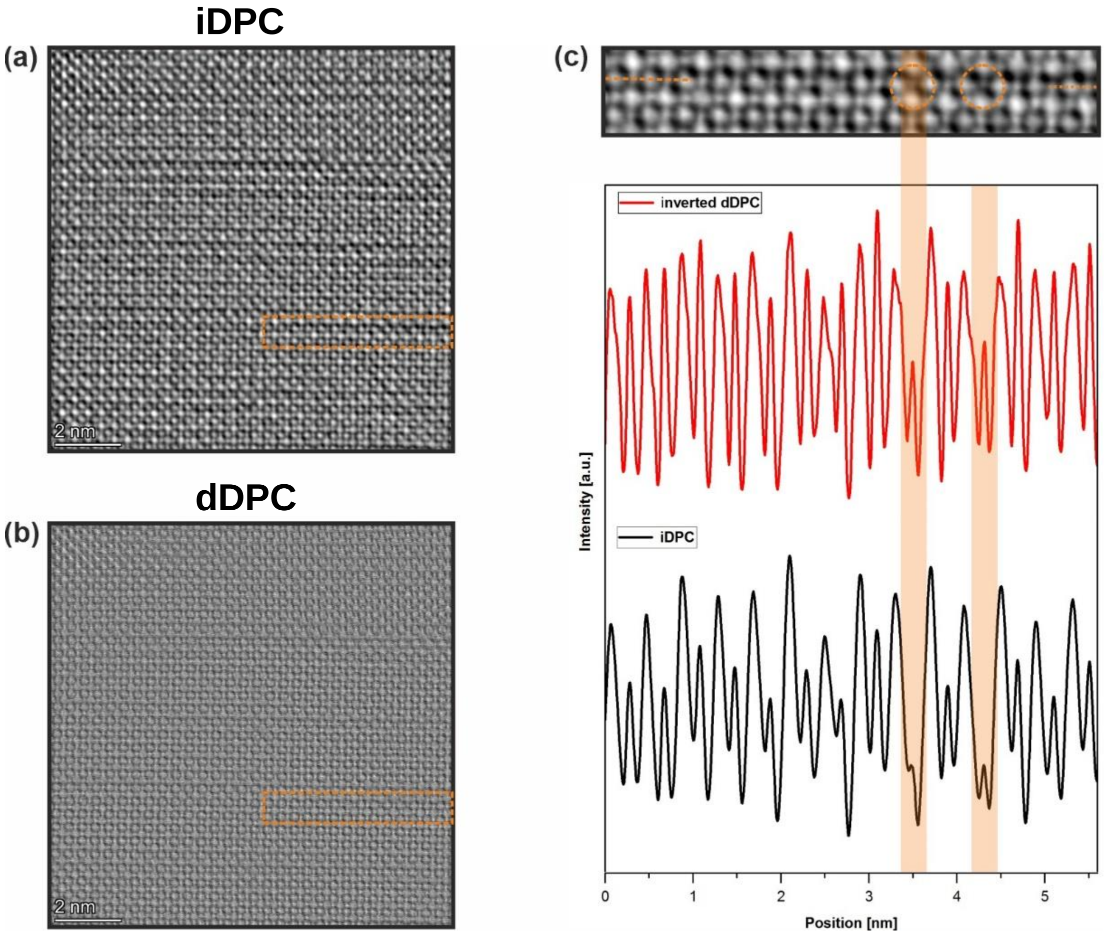

Summary

DPC STEM is a very intriguing microscopy technique, capable of imaging electromagnetic fields.

By combining DPC STEM with other well known imaging and spectroscopic techniques new insights into the relationship of chemical structure and physical properties can be gained

E.g. magnetic domain structure of spinodal alloys

iDPC ‚new‘ technique solving the problem of imaging light elements

Also defects can be imaged – maybe also useful for quantification?

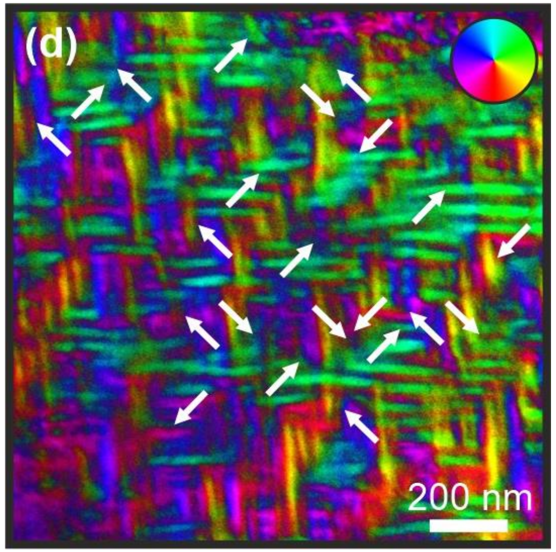

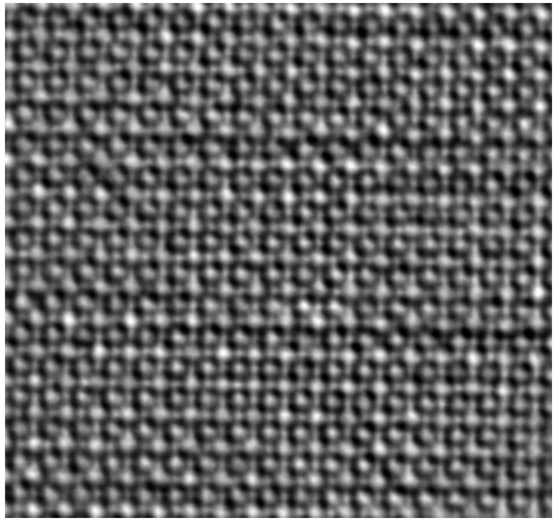

Acknowledgement

TU Graz:

	Felmi-ZfE:	F. Hofer, M. Dienstleder, D. Knez, G. Haberfehlner, J. Lammer, M. Nachtnebel, R. Winkler, H. Plank, G. Kothleitner
	IMAT:	S. Arneitz, Prof. C. Sommitsch
KFU Graz:		P. Knoll, S. Topolovec (TU)
Univ. Regensburg:		Prof. J. Zweck
Univ. Leoben:		J. Lie, U. Haselmann, Z. Zhang
ThermoFisherScientific:		D. Klenov, S. Lazar

Appendix

Advanced STEM

HR Spectroscopy:

HAADF

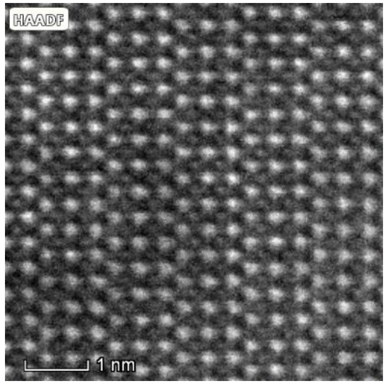

EDXS

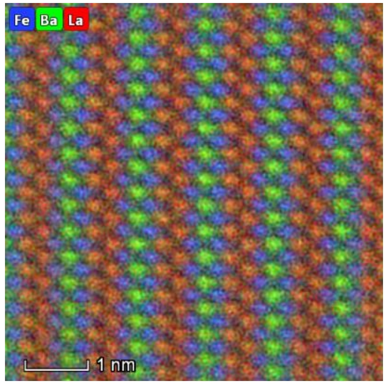

EELS

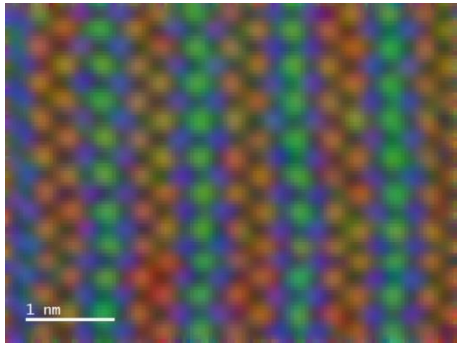

Measurements / results of Judith Lammer [1]

Tomography:

- Mg
- Mg+0
- Ti (+B)
- Ag (+Mg)
- Cu

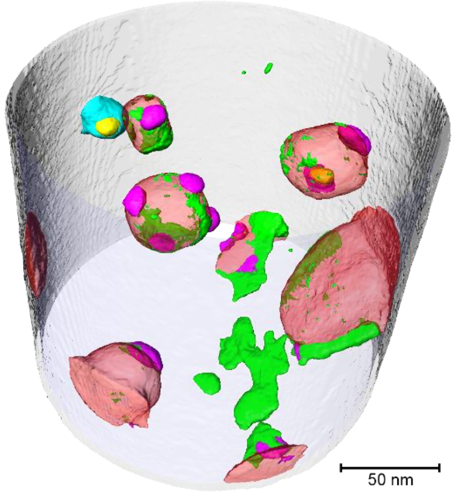

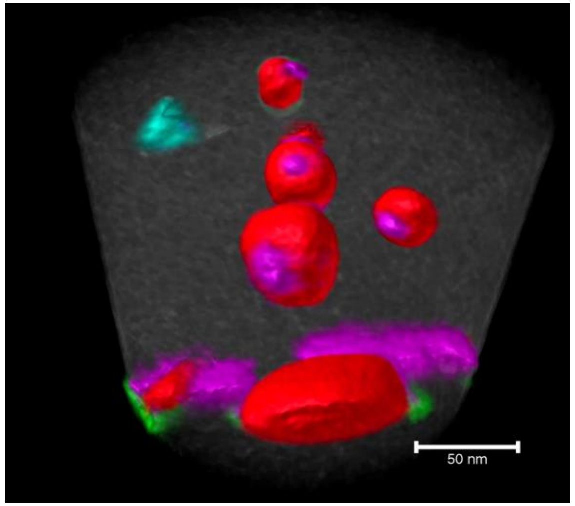

Measurements / results by Georg Haberfehlner

In-situ:

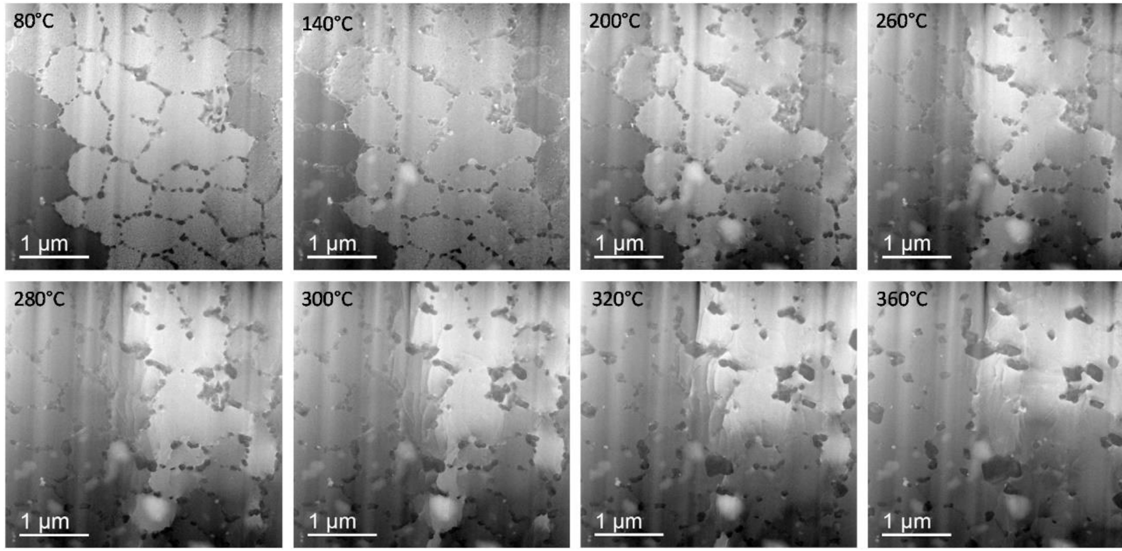

Measurements / results of Mihaela Albu [2]

[1] Lammer et al. *Ultramicroscopy 234* (2022)
[2] Albu et al. *Additive Manufacturing 36* (2020)

Examples of magnetic specimen

‚Visualizing‘ the movement of the e-beam

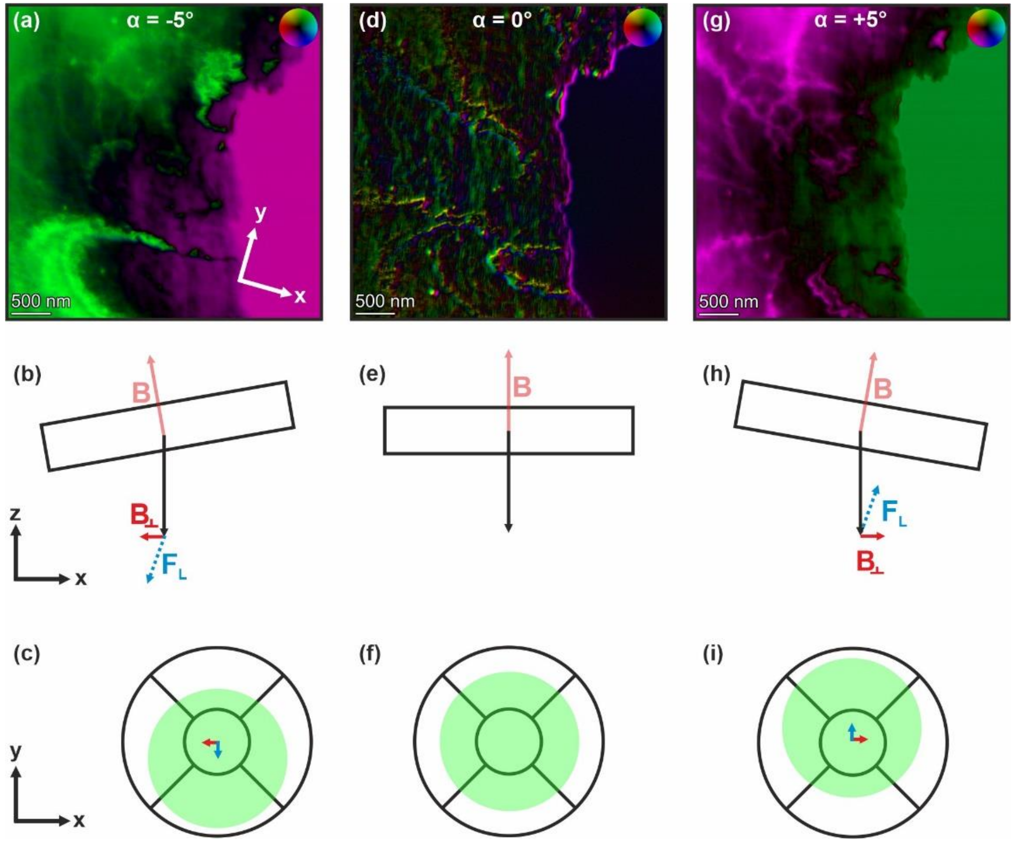

Magnetic DPC tilt-series of polycrystalline thin Co-film

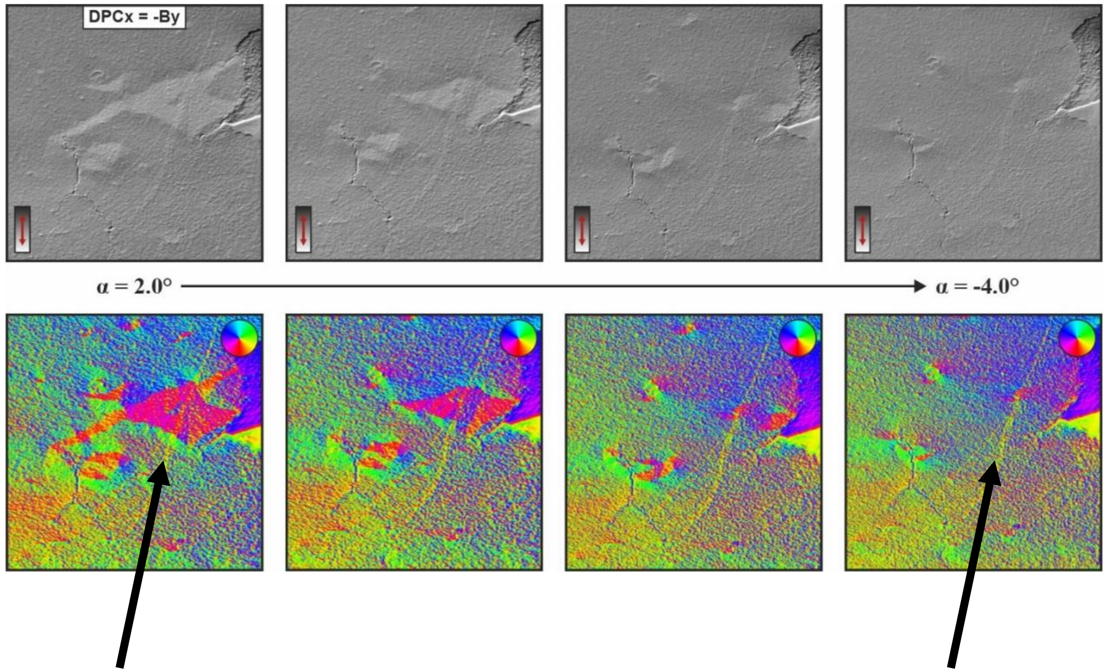

Magnetic domains flip due stray field within the microscope

Integrated DPC

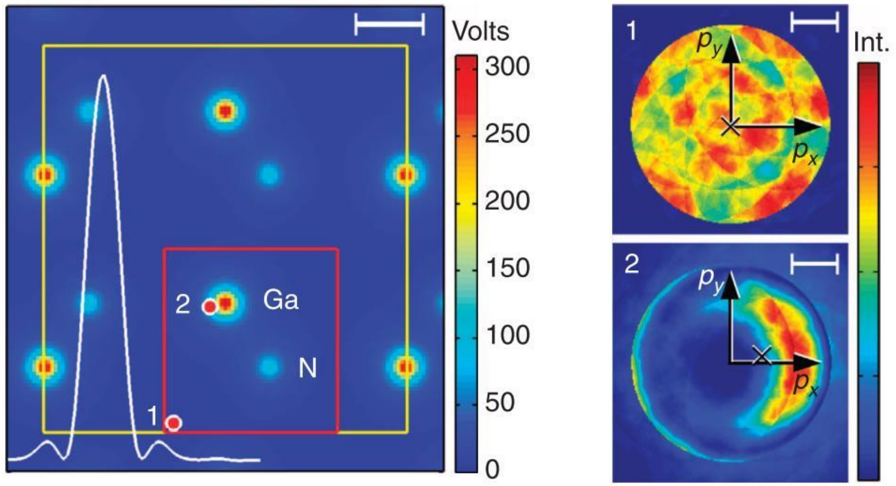

Image from Müller et al. [11]

Near an atomic column, the electrostatic potential is not homogeneous across the diameter of the electron beam!

Rigid-disk-shift model inappropriate and QM wave approach to calculate $< \hat{p} >$ is necessary

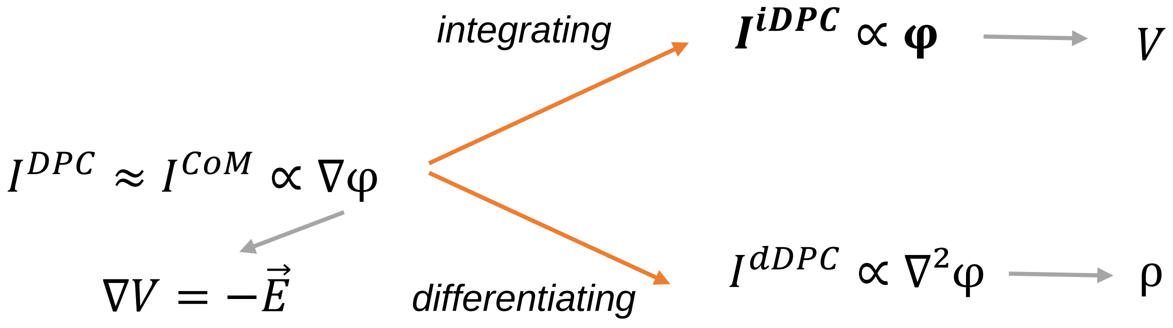

The iDPC image is a direct map of the electrostat. Potential

The dDPC image is a direct map of the charge density distr.

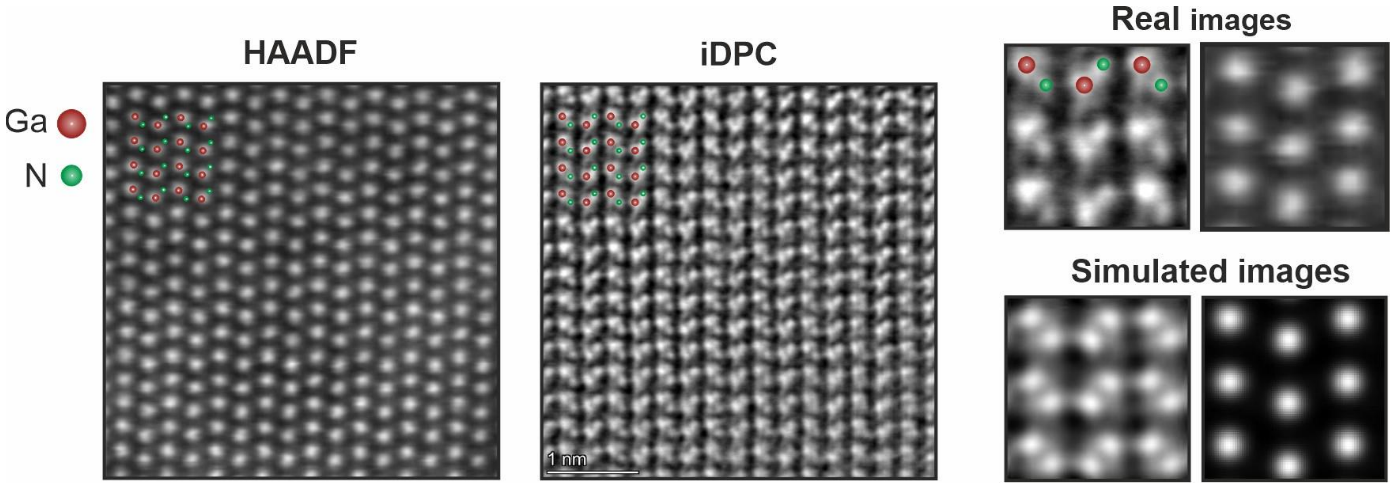

[11] Müller et al. *Nature communications 5* (2014)

$Cu_{52}Ni_{34}Fe_{14}$ – MFM

AFM/MFM principle

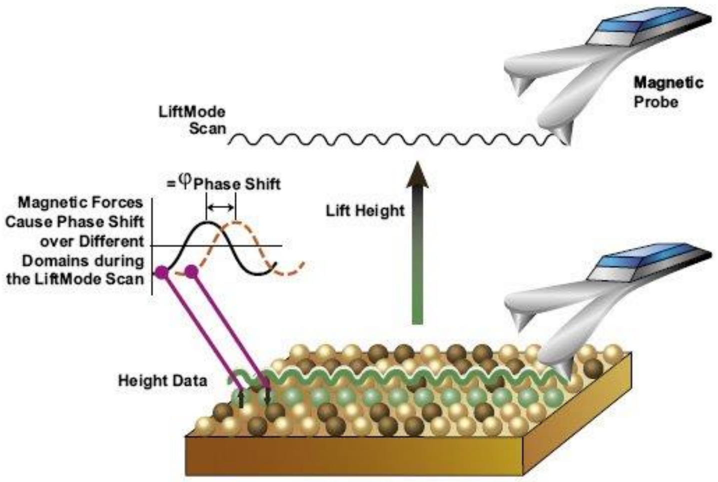

* Image from: https://blog.brukerafmprobes.com/guide-to-spm-and-afm-modes/magnetic-force-microscopy-mfm/

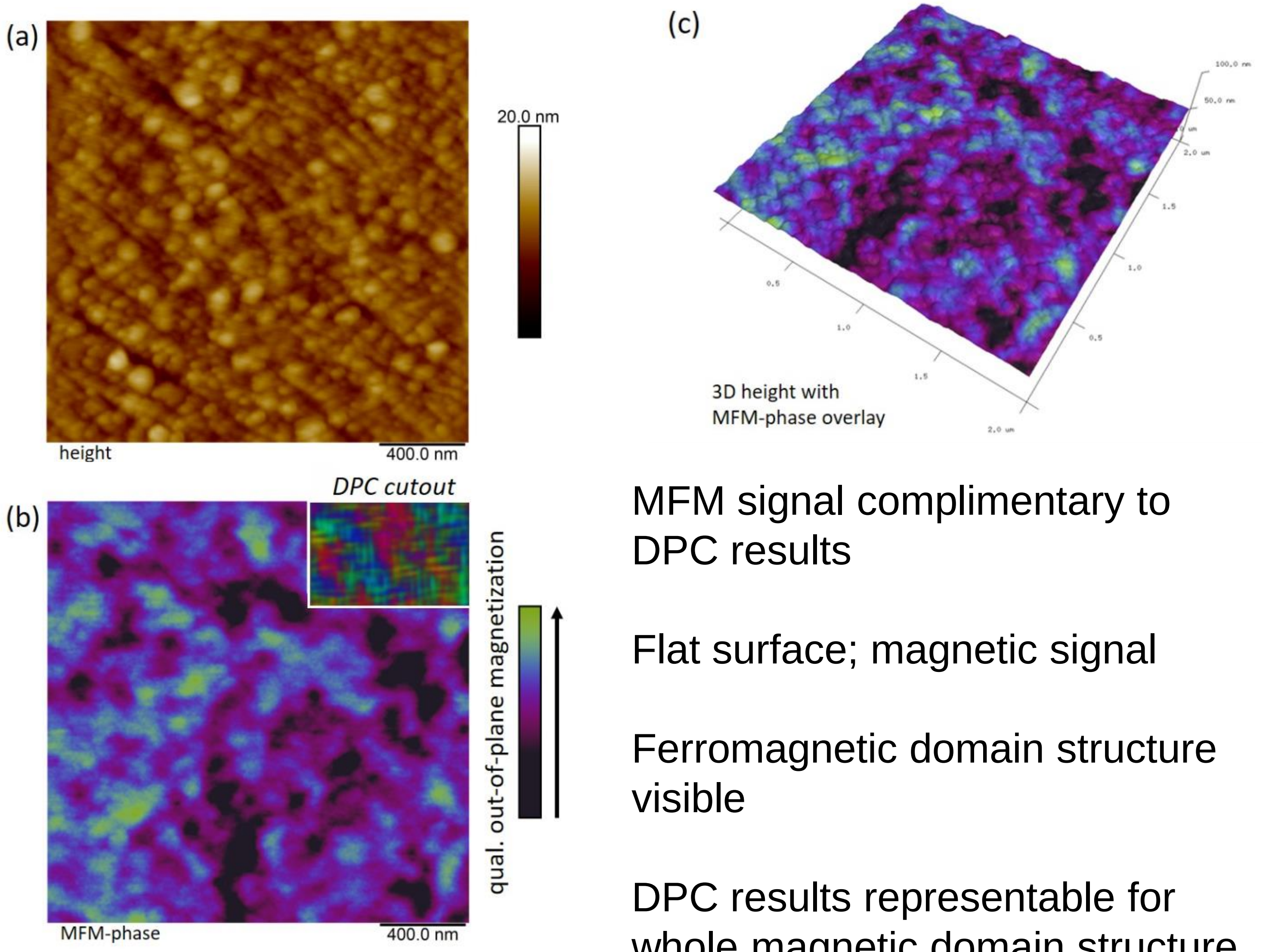

MFM signal complimentary to DPC results

Flat surface; magnetic signal

Ferromagnetic domain structure visible

DPC results representable for whole magnetic domain structure

Challenges of DPC measurements

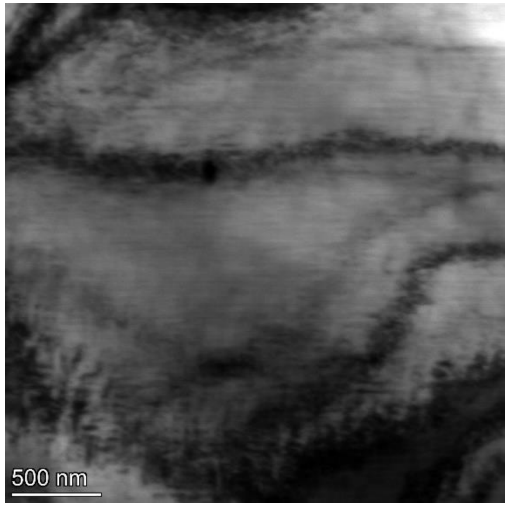

Dynamical scattering effects (diffraction contrast, channeling effects)

Topographic effects that may lead to misinterpretation (wedge, contaminations, $\varphi = \varphi(r)$)

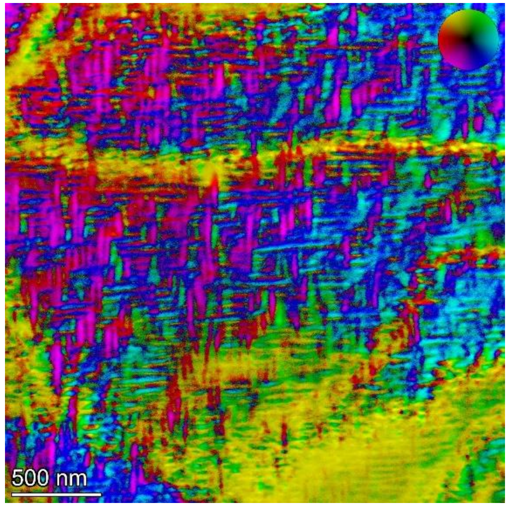

Stray fields, e.g. magnetic stray fields of lenses, ~10 kA/m (100-150 Oe) along optic axis

Stability of microscope

Superposition of electric and magnetic fields

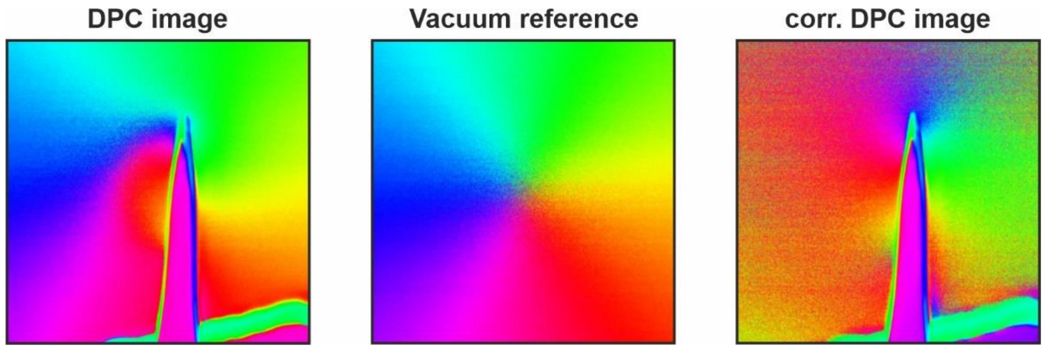

[19] Seki et al. *Microscopy 70* (2021)
[20] Zweck et al. *Ultramicroscopy 168* (2016)

Challenges of DPC

DPC very sensitive to abberations

Thickness limitations (POA valid for few nm!)

Image simulations (multi-slice) needed to understand contrast of ‚thick' specimens

Limitations due to 4-quadrant detector – signal across one segment gets summed up – information about distribution within segment ist lost

‚Limited' to post-acquisition processing

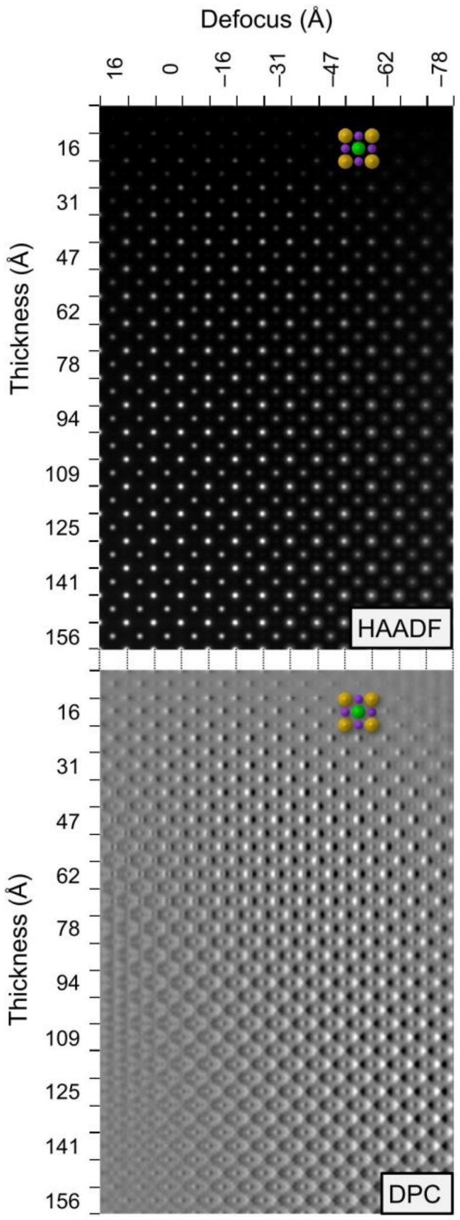

Image from Close et al. [20]

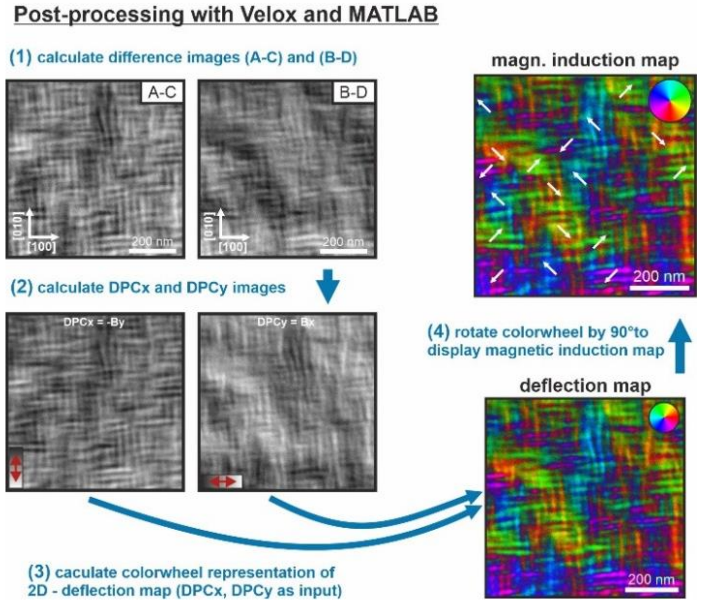

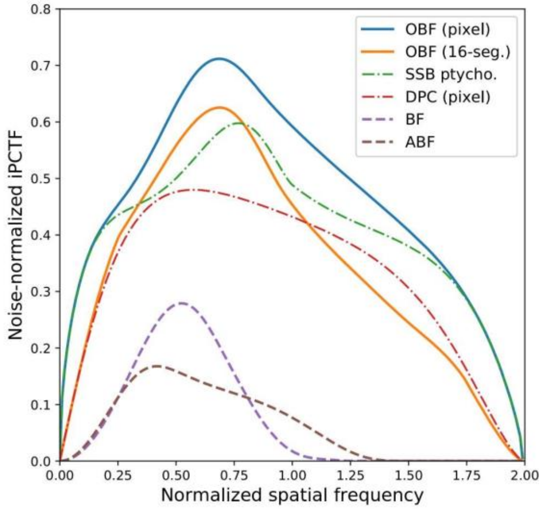

Image from Ooe et al. [21]

[20] Close et al. *Ultramicroscopy 159* (2015)
[21] Ooe et al. *Ultramicroscopy 220* (2021)